DOI: 10.1002/chem.201001330

In Situ Formation of Au–Pd Bimetallic Active Sites Promoting the Physically Mixed Monometallic Catalysts in the Liquid-Phase Oxidation of Alcohols

Di Wang,*[a, c] Alberto Villa,[a, d] Paolo Spontoni,[b] Dang Sheng Su,*[a] and Laura Prati[b]

Abstract: The catalytic oxidation of alcohols with molecular oxygen on supported nanometallic catalysts represents one of the green methods in a crucial process for the synthesis of fine chemicals. We have designed an experiment using physically mixed Au/AC and Pd/AC (AC = activated carbon) as the catalyst in the liquid-phase oxidation of benzyl alcohol by aerobic oxygen. The evolution of the physically mixed catalyst structures at different stages in the catalytic reaction was investigated by aberration-corrected high-resolution transmission electron microscopy and spatially resolved element mapping techniques at the nanometre scale, and they were also compared with the structure of the bimetallic alloy. For the first time we show the formation of surface Au–Pd bimetallic sites by reprecipitation of Pd onto Au nanoparticles. Negligible Au leaching was observed. The in situ structural evolution can be directly correlated to the great enhancement of the catalyst activity. Moreover, we distinguish the different behaviours of Au and Pd, thus suggesting an oxygen differentiating mechanism for Au and Pd sites. The findings are of great importance to both the understanding of the structure–activity correlation and the design of highly active catalysts in green chemistry.

Keywords: alloys · gold · nanostructures · oxidation · palladium

Introduction

The catalytic oxidation of alcohols with molecular oxygen instead of stoichiometric amounts of inorganic or organic oxidants is a crucial process for the synthesis of fine chemicals.[1] In the last decades, research has clearly started to focus on green methods using "clean" (i.e., producing bio-compatible co-products such as H_2O) oxidants such as H_2O_2 and preferably O_2 with the use of supported metal nanoparticles as the catalyst.[1a,2] Compared to monometallic catalysts, in many cases, bimetallic systems showed an improved activity and selectivity.[3,4] During the catalytic oxidation of alcohols, a synergistic effect between gold and other metals, such as Pd and Pt, has been observed.[3]

In particular, Au–Pd and Au–Pt, with respect to their monometallic counterparts, show an extra high activity and high resistance to deactivation due to synergistic effects.[3a,c,5] In our previous work, a well-defined alloy phase and homogeneously dispersed Au–Pd bimetallic catalyst supported on activated carbon (AC) was successfully synthesised and tested in liquid-phase selective oxidation of alcohols and polyols.[3b,6] The promotion effect therefore can be directly correlated to an Au–Pd synergistic effect. Subsequently, series of catalysts were prepared with different Au/Pd ratios, thereby suggesting that the surface Pd monomer in contact with Au has a prominent promoting effect on the activity[7] and stability, particularly reducing the leaching of Pd.[8] Moreover, experiments on physically mixed Au and Pd supported on AC revealed that there was an active role of both metals.[9] To study this aspect in more detail and to evidence the role of Au, Pd and Au–Pd bimetallic sites during the reaction, we designed an experiment using physically mixed Au/AC and Pd/AC as catalyst for the liquid-phase oxidation

[a] Dr. D. Wang, Dr. A. Villa, Dr. D. S. Su
Department of Inorganic Chemistry
Fritz Haber Institute of the Max Planck Institute
Faradayweg 4–6, 14195 Berlin (Germany)
Fax: (+49) 7247-82-8976
Fax: (+49) 30-8413-4405
E-mail: di.wang@kit.edu
dangsheng@fhi-berlin.mpg.de

[b] P. Spontoni, Prof. L. Prati
Dipartimento CIMA L.Malatesta, Università di Milano
via Venezian 21, 20133 Milano (Italy)

[c] Dr. D. Wang
Current address:
Institut für Nanotechnologie, Karlsruher Institut für Technologie
Hermann-von-Helmholtz-Platz 1
76344 Eggenstein-Leopoldshafen (Germany)

[d] Dr. A. Villa
Current address:
Dipartimento CIMA L.Malatesta, Università di Milano
via Venezian 21, 20133 Milano (Italy)

of benzyl alcohol, to compare its performance with that of the bimetallic Pd@Au/AC alloy catalyst. The evolution of the physically mixed catalyst structures at different stages in the catalytic reaction was investigated by aberration-corrected high-resolution transmission electron microscopy (HRTEM)[10] and spatially resolved element mapping techniques, and they were also compared with the structure of the bimetallic alloy. We show that alloy formation also occurred during the reaction using a physical mixture of Au/AC and Pd/AC as catalyst. The in situ alloy formation clearly suggests that a dissolution/reprecipitation mechanism is present although no apparent leaching of metal occurred. Transmission electron microscopy (TEM) analysis versus reaction time allows the spatial evolution of metal nanoparticles to be determined, thus clarifying the role of Au and Pd in the alloy formation. The correlation between the structures of the catalysts and the reaction profile reveals the unexpected different behaviours of supported Au and Pd nanoparticles in the liquid-phase reaction, which provides a fundamental understanding of the role of Au and Pd and therefore the synergistic effect of the bimetallic catalyst and the mechanism of the liquid-phase oxidation of alcohols.

Results and Discussion

Figure 1 shows the profiles of conversion versus time for the oxidation of benzyl alcohol in water in the absence of a base. The AuPd alloy and, surprisingly, also the physical mixture Au/AC+Pd/AC showed higher activity than the

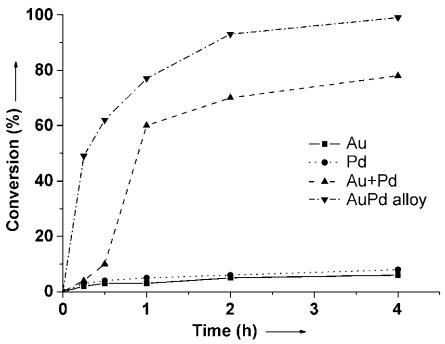

Figure 1. Profiles of conversion versus time for physically mixed Au/AC and Pd/AC, corresponding Pd/AC and Au/AC monometallic catalysts and the bimetallic 4Pd@6Au/AC (molar ratio of Pd/Au = 4:6) in the liquid-phase oxidation of benzyl alcohol.

single Au and Pd monometallic catalysts. After 0.5 h of reaction, Au and Pd showed, as expected, a very low activity (rate of consumption of benzyl alcohol [mol h^{-1} mol^{-1}] (BCR) of 3 and 15 h^{-1}, respectively): the Au catalyst because of the absence of the promotion of a base and the Pd because of rapid deactivation.[1a] The Au/AC+Pd/AC physical mixture showed a better activity (BCR of 28 h^{-1}) than that expected (BCR 8 h^{-1}) calculated on the basis of the proportional contribution of single Au and Pd in a 6:4 ratio. Alloyed AuPd showed an extra high activity (BCR of 988 h^{-1}) as already evidenced.[3b,6a] Interestingly, the physically mixed Au+Pd catalyst showed a prominent increase in conversion compared with the monometallic catalysts, though it is less active than the alloyed catalyst with the same Au/Pd ratio. In particular, from 0.5 to 1 h, the activity of the physically mixed catalyst increases drastically, which is largely different from the performance of the alloyed bimetallic catalyst. In terms of selectivity, all the catalysts showed a selectivity to benzaldehyde higher than 95%.

Electron microscopy is widely applied in the characterisation of catalysts to obtain knowledge about the complexity of nanoparticles structures, for example, their size, shape, surface decoration, and uncoordinated sites.[11] In the case of bimetallic nanocatalysts, the distribution of the different metals within the individual particle, which may lead to an alloy, core–shell structure, or segregations, modifies the structural configuration and electronic property considerably. With aberration-corrected HRTEM, the atomic configuration of nanoparticles can be determined with much more precision and confidence than ever before. Moreover, in scanning transmission electron microscopy (STEM) mode, energy-dispersive X-ray (EDX) spectrum imaging can be acquired with an electron probe size of about 1 nm, still allowing enough X-ray counts. Such high spatially resolved spectrum imaging can offer valuable information about the interior composition and configuration within single nanoparticles.

TEM observations confirmed the monometallic nature of the fresh physically mixed catalyst. Only pieces of activated carbon with monometallic Au or Pd were found. The average particle size of Au is larger than that of Pd and the distribution of the Au particle size covers a wider range than that of Pd. This is in good agreement with our TEM observation of Au/AC and Pd/AC before mixing. Figure 2a and b

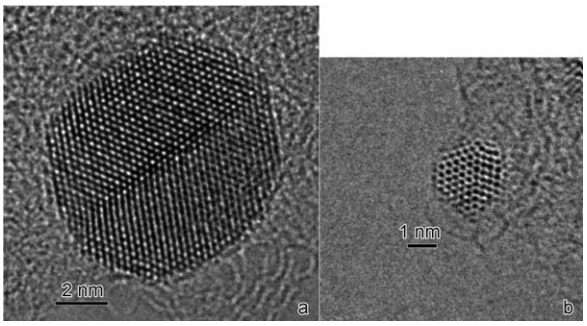

Figure 2. HRTEM images of a) one Au and b) one Pd particle on the activated carbon support in the physically mixed catalyst before reaction.

show representative HRTEM images of one Au and one Pd particle, respectively. Frequently, multiply twinned structures were observed for both monometallic particles, such as decahedrons and icosahedrons. After half an hour reaction of the oxidation of benzyl alcohol, the catalyst was removed from the reactor. After being filtered, washed and dried

under vacuum at room temperature, the catalyst was examined under an electron microscope (FEI Titan 80-300) by EDX spectrum imaging in STEM mode. The microscope was operated at an accelerating voltage of 300 kV. By acquiring EDX spectra from different pieces of activated carbon, we could determine whether it was the original Au/AC or Pd/AC. The spectrum imaging from these two different areas shows very interesting differences. We found a certain degree of Pd migration onto Au/AC and almost all the original monometallic Au particles now contained Pd. From spectrum imaging, for each scanned pixel the characteristic X-ray counts across the energy windows corresponding to Au M and Pd L excitations were integrated and the integrated counts were represented by intensities on each pixel, thus Au and Pd maps were extracted. Figure 3a shows the results of the EDX spectrum imaging on a few particles from one piece of original Au/AC in the physically mixed catalyst after 0.5 h reaction. It includes the STEM image, Au and Pd maps and the two maps superimposed. Due to the relatively weak signal of Pd, the intensities within each element map are only normalised to the maximum integrated counts of the corresponding element excitation (Au M or Pd L) and therefore do not represent the element concentration. The integrated spectrum of all the pixels in the scanned area is shown in Figure 3b. It clearly indicates the migration of Pd atoms onto the Au particles, thereby forming bimetallic particles. The quantitative analysis of the integrated spectrum using Au L and Pd L excitations suggests a Au/Pd atomic ratio of 96.6:3.4. To inspect the homogeneity of the formed bimetallic particles, EDX spectra were integrated from the individual particles in the map shown in Figure 3a and other maps from the same sample (not shown in this paper). The quantification results are plotted in Figure 3b as well. For the mixed catalyst after 30 min reaction, the Pd concentration is much higher for the particle smaller than 3 nm. It is quite understandable that at the beginning the same deposition rate of Pd will lead to a high Pd ratio on extra-small particles.

The EDX spectrum imaging from a piece of original Pd/AC is shown in Figure 4a. By comparing the Au and Pd maps, the inhomogeneous distribution of the two metals could be readily seen. By referring to the corresponding STEM image, a big particle and a small one located above and to the left to it were found to be Au-rich; Pd also exists on these particles. Clearly, the original Au particle, which was weakly adhered to the activated carbon support, may detach from the support and fall onto a piece of Pd/AC. Like other Au particles, during the reaction, Pd was also redeposited onto Au, thereby forming bimetallic particles. In contrast, the Pd particles remained almost monometallic and very little Au was found to be redeposited onto Pd particles, as shown in the superimposed Au and Pd map. The EDX spectra were integrated from the two areas indicated by rectangles in the STEM image and are shown in Figure 4b and c, respectively. The spectrum from the original big Au particle suggests that it contains both Au and Pd, whereas the one on the original Pd particle shows no detectable Au by EDX. These results from the spectrum imaging on Au/AC and Pd/AC pieces clearly indicates the migration of Pd onto Au particles, but very little migration of Au. Only some Au particles were observed to fall onto the activated carbon supporting the Pd particles. These particles were also found to be bimetallic.

Similar spectrum imaging results were obtained from the catalyst after oxidation of benzyl alcohol for one hour. Figure 3c shows the STEM image, Au and Pd maps and the two superimposed maps of a few particles from one piece of original Au/AC in the catalyst after one hour of reaction. The integrated spectrum of all the pixels in the scanned area is shown in Figure 3d. All the Au particles were found to have Pd atoms deposited onto them, thus forming bimetallic particles. The quantitative analysis of the integrated spectrum suggests a Au/Pd atomic ratio of 91.9:8.1. Figure 3d also shows the Pd concentration for individual particles from the map in Figure 2c and other maps from the same sample. After 1 h reaction, the dependence of Pd concentration on the particle size is not obvious and the Pd ratio fluctuates from particle to particle. With longer reaction time, it is clear that there is more Pd deposited on Au but at the same time, those Pd atoms on small particles without enough stabilisation by Au could undergo leaching again, therefore there is less dependence of the Pd ratio on particle size. The STEM image, Au and Pd maps and the superimposed map from a piece of original Pd/AC are shown in Figure 5a. A big particle was found to consist of both Au and Pd but Au forms the majority. This particle came from the original Au/AC piece. Other particles were dominated by Pd. The EDX spectra were integrated from two of the particles in the rectangular areas in the STEM image and are shown in Figure 5b and c, respectively. The spectra clearly indicate that similarly to the catalyst after 0.5 h reaction, the Pd particles contain no detectable Au after 1 h reaction.

However, the element distribution within the formed bimetallic particle is still not clear. In particular, whether the deposited Pd atoms segregate on the surface of the Au particles or diffuse into the Au particles is of great importance since the specific bimetallic configuration will determine the surface chemistry of the particle. Therefore we acquired a high-angle annular dark field (HAADF) STEM image of a single particle with atomic resolution to clarify this problem. The contrast of the HAADF STEM image is known to be proportional to the integrated Z^2 (Z = atomic number of the atom) along the incident electron direction. Figure 6a shows the HAADF STEM image of one Au–Pd bimetallic particle in the catalyst after 0.5 h reaction. The EDX spectrum from the exact same particle is shown in Figure 6b. Quantitative analysis of this spectrum gives an atomic ratio of Au/Pd = 96.1:3.9, which is very close to the average level obtained from the integrated spectrum in Figure 3b. From the lattice displayed in the image, it can be deduced that the particle has a single-crystalline structure and no segregated Pd clusters on the Au particle surface were observed. Pd atoms diffuse into the Au lattice both on the surface and probably also into the sub-surface layers. Our observation is in very

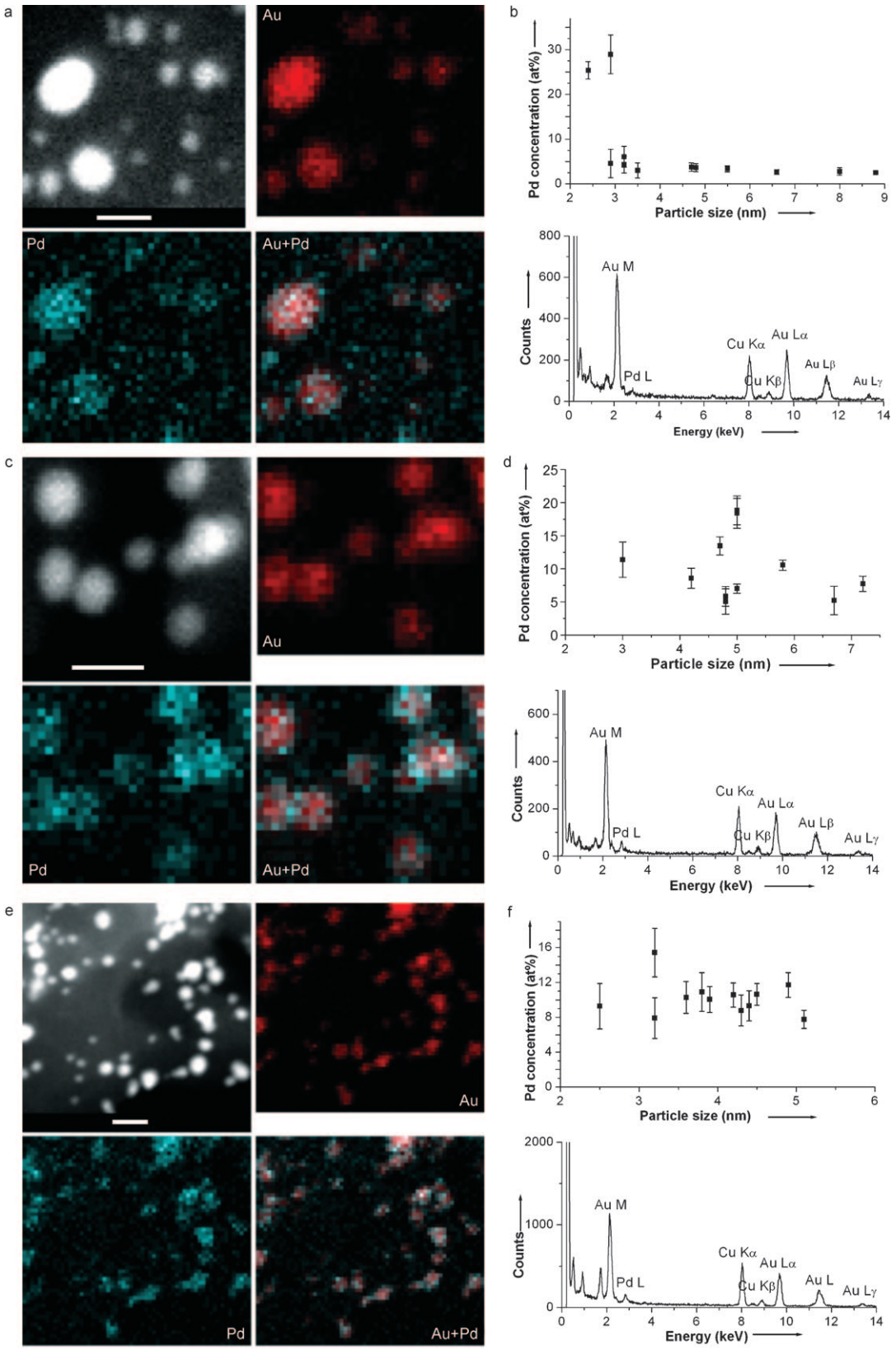

Figure 3. STEM images, Au and Pd maps and the two superimposed maps from one piece of original Au/AC in the physically mixed catalyst after a) 0.5 and c) 1 h of benzyl alcohol oxidation. b) Pd concentration of the particles shown in map (a) and the other maps from the same sample as well as the integrated EDX spectrum from the whole scanned region in map (a). d) Pd concentration of the particles shown in map (c) and the other maps from the same sample as well as the integrated EDX spectrum from the whole scanned region in map (c). e) STEM image, Au and Pd maps and the two superimposed maps from the bimetallic Pd@Au/AC catalyst with a molar ratio of Pd/Au = 4:6. f) Pd concentration of the particles in map (e) and the other maps from the same sample as well as the integrated EDX spectrum from the whole scanned region in map (e). The scale bars in all the STEM images are 10 nm.

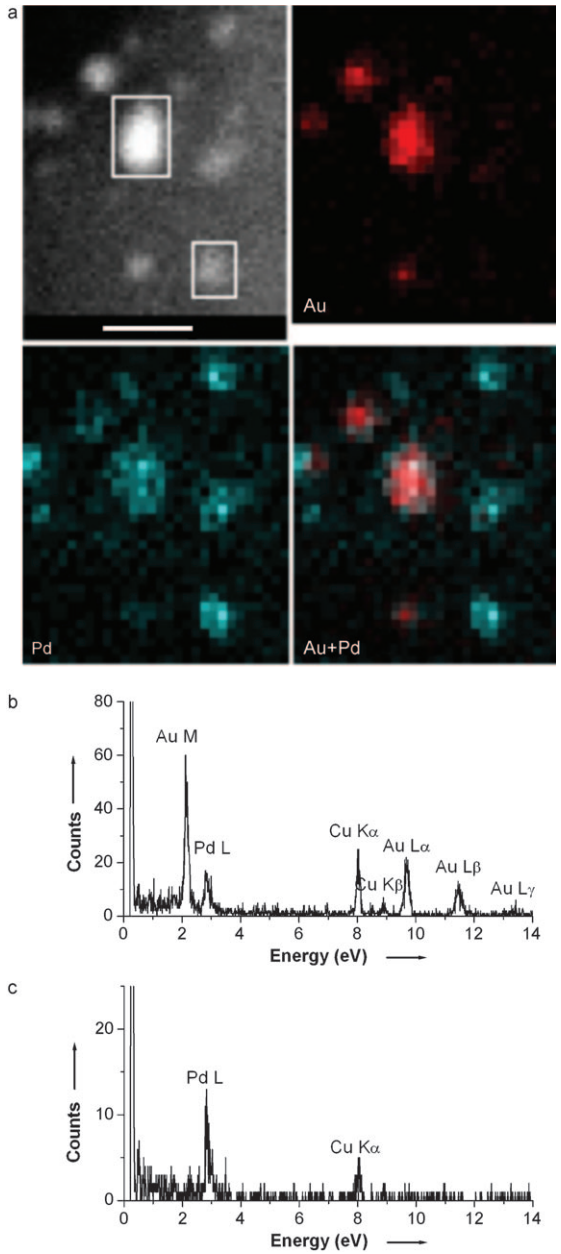

Figure 4. a) STEM image, Au and Pd maps and the two superimposed maps from one piece of original Pd/AC in the physically mixed catalyst after 0.5 h reaction of benzyl alcohol oxidation. b) and c) The integrated EDX spectra from the two areas indicated by a big and a small rectangle in the STEM image in (a), respectively, which suggests that the original big Au particle contains both Au and Pd, whereas there is no detectable Au on the original Pd particle. The scale bars in all the STEM images are 10 nm.

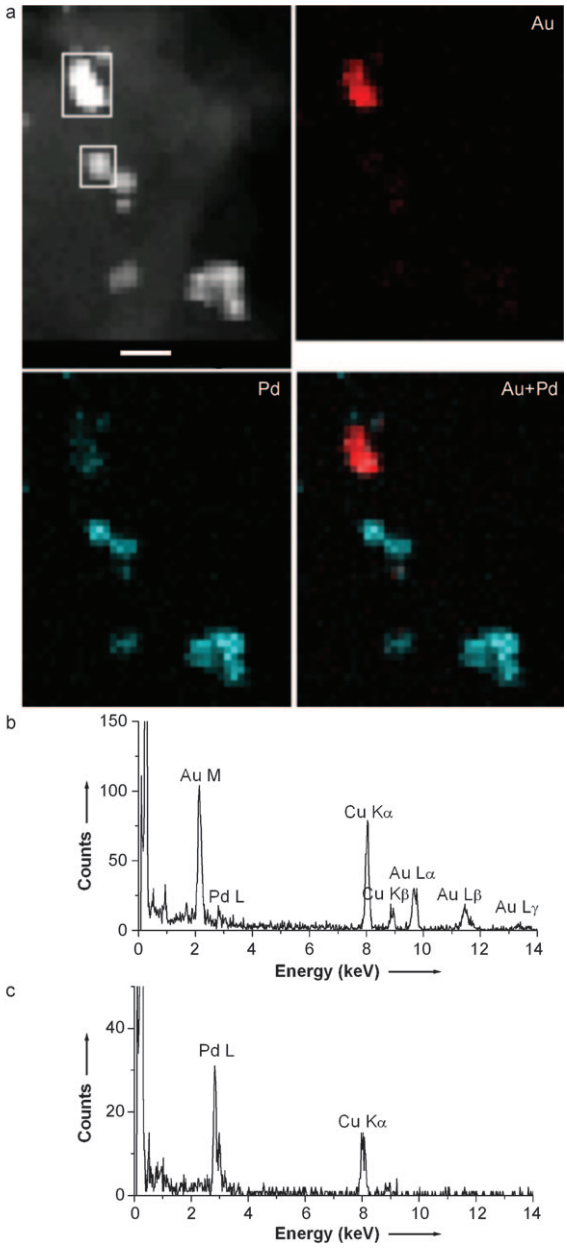

Figure 5. a) STEM image, Au and Pd maps and the two superimposed maps from one piece of original Pd/AC in the physically mixed catalyst after 1 h of benzyl alcohol oxidation. b) and c) The integrated EDX spectra from the two areas indicated by a big and a small rectangle in the STEM image, respectively, which suggests that the original big Au particle contains both Au and Pd, whereas there is no detectable Au on the original Pd particle. The scale bars in all the STEM images are 10 nm.

good agreement with the DFT calculation of the Pd atom added on the stepped (111) Au surface.[12] The DFT calculation suggests that the surface position by the step is the most unfavourable in energy, whereas the second and third sub-surface layers underneath the terrace are more favoured.

In comparison, we also acquired the EDX spectrum image of the bimetallic Pd@Au/AC catalyst[6a] with a molar ratio of Pd/Au = 4:6. The STEM image, Au and Pd maps, as well as superimposed map are shown in Figure 3e. The Pd concentration for individual particles of this sample and the integrated EDX spectrum are shown in Figure 3f. Clearly, the particles in the bimetallic catalyst are of a more uniform Au/Pd ratio. The integrated EDX spectra of single particles are similar to the integrated spectrum of the whole of the scanned area.[6a]

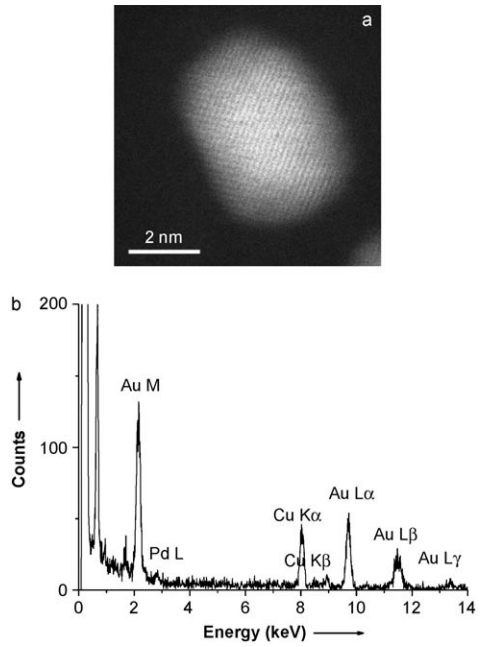

Figure 6. a) A HAADF STEM image of one Au–Pd bimetallic particle formed after 0.5 h of reaction. b) The EDX spectrum from the same particle. The particle has a single-crystalline structure and no segregation of Pd was observed.

By considering the EDX quantitative results, the trend of increasing Pd deposition on Au particles as the reaction progresses is clearly noticed. The increase of the Pd concentration is accompanied by an increase of the catalyst's activity. The present experiment using the physically mixed Au/AC and Pd/AC is in good agreement with our previous experiment on the effect of the Au/Pd ratio on the benzyl alcohol oxidation rate.[13] After half an hour of the reaction, though AuPd bimetallic particles begin to form, the Au/Pd ratio (96.6:3.4) is close to the Au-rich catalyst reported in reference [13] and the activity is still low. However, after one hour, the Au/Pd ratio (91.9:8.1) on the bimetallic particles is close to the most active ratio (8:2) reported in reference [13], which shows a distinct synergistic effect and high activity, and we did indeed observe a comparable performance.

Conclusion

In summary, we have observed the different behaviours of gold and palladium supported on activated carbon in the liquid-phase oxidation reaction that leads to the formation of surface AuPd bimetallic sites by migration of Pd onto Au nanoparticles. Soluble atomic Pd species (like Pd^{2+}) can then reprecipitate on Au-supported nanoparticles to form alloyed species. Negligible Au leaching was observed. Some Au particles only detach from the AC support and fall onto other pieces of AC; this process does not produce an alloy. Moreover, this finding casts new light on the mechanism of liquid-phase oxidation with oxygen differentiating whether the mechanism acts with the Pd or Au catalyst. In fact, the leaching of atomic Pd is in agreement with a mechanism that involves the dehydrogenation of the alcohol coordinated to a cationic species of Pd, followed by oxidation of the surface hydride with oxygen to form water.[3a] With Au, on the contrary, the involvement of soluble atomic species seem to be avoided, which supports a different active mechanism where the rate-determining step involves a superoxo-like oxygen species adsorbed on Au.[14] When bimetallic sites are formed Au stabilises Pd atoms, thereby preventing Pd aggregation and leaching, which leads to deactivation of the catalyst.

Experimental Section

Materials used in catalyst synthesis and catalytic reaction included $NaAuCl_4 \cdot 2H_2O$ and Na_2PdCl_4 from Aldrich (99.99% purity), activated carbon from Camel (X40S; surface area (SA) = 900–1100 $m^2 g$; pore volume (PV) = 1.5 $mL g^{-1}$), $NaBH_4$ of purity > 96% from Fluka, and polyvinylalcohol (PVA; M_r = 13000–23000, 87–89% hydrolyzed) from Aldrich. A 2 wt% solution of PVA in water was prepared. Gaseous oxygen from SIAD was 99.99% pure.

To prepare the Au sol, solid $NaAuCl_4 \cdot 2H_2O$ (0.043 mmol) and PVA (2 wt%) solution (1.64 mL) were added to H_2O (130 mL). After 3 min, an $NaBH_4$ (0.1 M) solution (1.3 mL) was added to the yellow solution under vigorous magnetic stirring. The ruby red Au^0 sol formed immediately.

To prepare the Pd sol, aqueous Na_2PdCl_4 stock solution (0.043 mmol) and PVA (2 wt%) solution (880 mL) were added to H_2O (130 mL). After 3 min, a $NaBH_4$ (0.1 M) solution (860 mL) was added under vigorous magnetic stirring. The brown Pd^0 sol formed immediately.

Monometallic Au/AC and Pd/AC were synthesised following the procedure described elsewhere,[1c] with 1 wt% metal loading. Within a few minutes of sol generation, the colloid (acidified to pH 2 by sulfuric acid) was immobilised by adding the activated carbon under vigorous stirring. The amount of support was calculated as having a total final metal loading of 1 wt%. After 2 h the slurry was filtered, the catalyst was washed thoroughly with distilled water (neutral mother liquors) and dried at 100 °C for 4 h. ICP analyses were performed on the filtrate using a Jobin Yvon JV24 to verify the metal loading on the support. The physically mixed catalyst was prepared by mixing Au/AC with Pd/AC in an Au/Pd molar ratio of 6:4.

Bimetallic catalysts were prepared following the procedure reported in reference [6a]. $NaAuCl_4 \cdot 2H_2O$ (0.072 mmol) was dissolved in H_2O (140 mL), and PVA (2%, w/w) was added (0.706 mL). The yellow solution was stirred for 3 min, after which 0.1 M $NaBH_4$ (2.15 mL) was added under vigorous magnetic stirring. The ruby-red Au^0 sol formed immediately. Within a few minutes of sol generation, the gold sol was immobilised by adding the support (acidified to pH 2 by sulfuric acid) under vigorous stirring. The amount of support was calculated as having a gold loading of 0.73 wt%. After 2 h, the slurry was filtered and the catalyst was washed thoroughly with distilled water (neutral mother liquors). The Au/AC was dispersed in water (140 mL), and Na_2PdCl_4 (10 wt% in Pd solution; 0.0386 mL) and PVA solution (0.225 mL) were added. H_2 was bubbled (50 mL min^{-1}) through the mixture under atmospheric pressure and at room temperature for 2 h. After an additional 18 h, the slurry was filtered and the catalyst was washed thoroughly with distilled water. Inductively coupled plasma mass spectrometry (ICP-MS) analyses were performed on the filtrate using a Jobin Yvon JV24 instrument to verify the metal loading on the support. The total metal loading was 1 wt%.

The catalysts were tested in the oxidation of benzyl alcohol in pure water. Reactions were carried out in a thermostatted glass reactor (30 mL) and with an electronically controlled magnetic stirrer connected

to a large reservoir (5000 mL) containing oxygen at 1.5 atm. The oxygen uptake was followed by a mass flow controller connected to a PC through an A/D board, which plotted a flow–time diagram. The alcohol (0.3 M) and the catalyst (substrate/metal = 500 mol/mol) were mixed in distilled water (total volume 10 mL). The reactor was pressurised at 1.5 atm of O_2 and thermostatted at 60 °C. Once the required temperature was reached, the gas supply was switched to oxygen and the monitoring of the reaction started. The reaction was initiated by stirring. For the identification and analysis of the products a GC–MS and GC (a Dani 86.10 HT gas chromatograph equipped with a capillary column (BP21 30 m × 0.53 mm), 0.5 μm film, made by SGE), were used for comparison of the authentic samples. For the quantification of the reactant–products the external calibration method was used. The physically mixed catalyst was prepared by mixing 1% Au/AC with 1% Pd/AC in a Au/Pd molar ratio of 6:4.

The catalysts were examined by using a FEI Titan 80-300 electron microscope equipped with a CEOS image spherical aberration corrector, Fischione model 3000 HAADF STEM detector and EDAX SUTW EDX detector. The microscope was operated at an accelerating voltage of 300 kV in TEM mode for HRTEM and in STEM mode for STEM and EDX spectrum imaging. The probe size was about 1 nm as a good compromise of spatial resolution and beam current. Therefore for each spectrum image, the pixel size was also 1 nm. The pixel sizes of the spectrum images were 40 × 37, 30 × 26 and 60 × 55 for Figure 2a, c and e, respectively. The dwell time per pixel was 3 s. The specified probe current for a 1 nm probe is ≥ 0.6 nA. Since the probe size in our experiment was about 1 nm, the current should be similar to the specified value. The element maps were generated by integrating the Au M and Pd L intensities, respectively. The quantification was carried out using Au L and Pd L lines processed by using the TIA software.

Acknowledgements

The authors acknowledge DAAD and CRUI for the financial support of the personnel exchange program.

[1] a) T. Mallat, A. Baiker, *Chem. Rev.* **2004**, *104*, 3037; b) M. S. Sigman, D. R. Jensen, *Acc. Chem. Res.* **2006**, *39*, 221; c) R. A. Sheldon, I. W. C. E. Arends, G.-J. ten Brink, A. Dijksman, *Acc. Chem. Res.* **2002**, *35*, 774.

[2] a) R. A. Sheldon, I. W. C. E. Arends, A. Dijksman, *Catal. Today* **2000**, *57*, 157; b) M. Besson, P. Gallezot, *Catal. Today* **2000**, *57*, 127.

[3] a) D. I. Enache, J. K. Edwards, P. Landon, B. Solsona-Espriu, A. F. Carley, A. A. Herzing, M. Watanabe, C. J. Kiely, D. W. Knight, G. J. Hutchings, *Science* **2006**, *311*, 362; b) N. Dimitratos, A. Villa, D. Wang, F. Porta, D. S. Su, L. Prati, *J. Catal.* **2006**, *244*, 113; c) C. L. Bianchi, P. Canton, N. Dimitratos, F. Porta, L. Prati, *Catal. Today* **2005**, *102*, 203–212.

[4] K. A. Kacprzak, L. Lehtovaara, J. Akola, O. Lopez-Acevedo, H. Häkkinen, *Phys. Chem. Chem. Phys.* **2009**, *11*, 7123.

[5] a) L. Guczi, *Catal. Today* **2005**, *101*, 53–64, and reference therein; b) W. Hou, N. A. Dehm, R. W. J. Scott, *J. Catal.* **2008**, *253*, 22; c) S. Demirel, K. Lehnert, M. Lucas, P. Claus, *Appl. Catal. B* **2007**, *70*, 637; d) S. Marx, A. Baiker, *J. Phys. Chem. C* **2009**, *113*, 6191–6201.

[6] a) D. Wang, A. Villa, F. Porta, D. S. Su, L. Prati, *Chem. Commun.* **2006**, 1956–1958; b) A. Villa, D. Wang, D. S. Su, G. M. Veith and L. Prati, *Phys. Chem. Chem. Phys.* **2010**, *12*, 2183.

[7] D. Wang, A. Villa, F. Porta, L. Prati, D. S. Su, *J. Phys. Chem. C* **2008**, *112*, 8617.

[8] A. Villa, D. Wang, N. Dimitratos, D. S. Su, V. Trevisan, L. Prati, *Catal. Today* **2010**, *150*, 8.

[9] W. C. Ketchie, M. Murayama, R. J. Davis, *J. Catal.* **2007**, *250*, 264.

[10] a) M. Haider, H. Rose, S. Uhlemann, B. Kabius, K. Urban, *J. Electron Microsc.* **1998**, *47*, 395; b) B. Freitag, S. Kujawa, P. M. Mul, J. Ringnalda, P. C. Tiemeijer, *Ultramicroscopy* **2005**, *102*, 209.

[11] a) S. Bernal, R. T. Baker, A. Burrows, J. J. Calvino, C. J. Kiely, C. J. López-Cartes, A. Pérez-Omil, J. M. Rodríguez-Izquierdo, *Surf. Interface Anal.* **2000**, *29*, 411–421; b) L. C. Gontard, L.-Y. Chang, C. J. D. Hetherington, A. I. Kirkland, D. Ozkaya, R. E. Dunin-Borkowski, *Angew. Chem.* **2007**, *119*, 3757; *Angew. Chem. Int. Ed.* **2007**, *46*, 3683–3685; c) P. L. Gai, E. D. Boyes, *Electron Microscopy in Heterogeneous Catalysis*, Taylor & Francis, New York, **2003**; d) D. S. Su, T. Jacob, T. W. Hansen, D. Wang, R. Schlögl, B. Freitag, and S. Kujawa, *Angew. Chem.* **2008**, *120*, 5083; *Angew. Chem. Int. Ed.* **2008**, *47*, 5005.

[12] S. Venkatachalam, T. Jacob, *Phys. Chem. Chem. Phys.* **2009**, *11*, 3263–3270.

[13] A. Villa, N. Janjic, P. Spontoni, D. Wang, D. S. Su, L. Prati, *Appl. Catal. A* **2009**, *364* 221.

[14] a) H. Tsunoyama, H. Sakurai, Y. Negishi, T. Tsukuda, *J. Am. Chem. Soc.* **2005**, *127*, 9374; b) M. Conte, H. Miyamura, S. Kobayashi, V. Chechik, *J. Am. Chem. Soc.* **2009**, *131*, 7189–7196.

Received: May 17, 2010
Published online: July 12, 2010

